J. Fluid Mech. (1971), *vol.* 49, *part* 3, *pp.* 577–591
Printed in Great Britain

Stability of vertical natural convection boundary layers: expansions at large Prandtl number

By C. A. HIEBER† AND B. GEBHART
Department of Thermal Engineering, Cornell University

(Received 2 September 1970)

Expansions are obtained for the large Prandtl number structure of the laminar natural convection boundary layer, together with its linear stability characteristics, for the case of a uniform-heat-flux semi-infinite vertical plate. The primary source of instability is shown to arise from a temperature-coupling effect associated with the inner heated region of the boundary layer. Based upon an empirical correlation between the results of linear stability theory and experimentally determined régimes of the turbulent-transition process, it is shown that the flow can be expected to become turbulent before the outer vorticity region of the laminar boundary layer is fully established. The results are generalized to the isothermal plate case.

1. Introduction

In a previous paper (Hieber & Gebhart 1971, hereafter referred to as (A)), numerical results were obtained for the linear stability of the natural convection boundary layer for the case of a semi-infinite vertical plate dissipating a uniform heat flux into a surrounding unbounded fluid. The amplification or decay of the arbitrarily small two-dimensional travelling wave disturbances was taken to be spatial. (As shown by Knowles & Gebhart (1968), a Squires theorem also applies to vertical natural convection boundary layers. It is noted that the theorem is not restricted to temporal, as opposed to spatial, amplification provided, in the latter instance, one assumes that the direction of maximum growth rate coincides with the direction of propagation of the three-dimensional travelling wave.) In particular, it was shown in (A) that, at large values of the Prandtl number (σ), the stability of the primary flow boundary layer is characterized by two distinct modes. One of these, mode I, was found to be related to the uncoupled (Orr–Sommerfeld) problem whereas the other, mode II, was seen to apparently arise directly from the coupling effect (i.e. the dependence of the disturbance velocity upon the disturbance temperature via buoyancy). Notably, it was found that mode II is much more unstable than mode I and that the non-dimensionalized frequencies associated with II are much larger than those of I.

In the present paper, the underlying physical effects characterizing modes I and II are determined in the limit of large σ. This is accomplished by means of asymptotic expansions for the primary flow and disturbance field as $\sigma \to \infty$.

† Present address: Clarkson College of Technology, Potsdam, New York.

As in (A), the analysis is for the case of the uniform-heat-flux semi-infinite vertical plate. The numerical technique employed is essentially the same as that in (A), the results being of comparable accuracy.

Results are presented in § 2 for the structure of the primary flow as $\sigma \to \infty$. Based upon the results of § 2, the large Prandtl number numerical results of (A) are recast in § 3 in terms of appropriately scaled (in σ) co-ordinates. These suggest the form of the asymptotic expansions (as $\sigma \to \infty$) for the disturbance field. Such expansions for modes II and I are presented in §§ 4 and 5, respectively. Some implications and generalizations of these results are then given in the concluding section, § 6.

2. The primary flow

Employing the same notation as in (A), we recall that the governing equations for the primary flow boundary layer are

$$F''' + 4FF'' - 3F'F' + H = 0, \tag{1}$$

$$H'' + \sigma(4FH' - F'H) = 0, \tag{2}$$

where $F(\eta)$ and $H(\eta)$ are the non-dimensionalized stream function and temperature (η being the 'similarity' variable, y/δ, where $\delta \equiv 5x/G^*$ characterizes the boundary-layer thickness when σ is $O(1)$ and where G^*, defined in (A), is proportional to the fourth-root of the Grashof number G), subject to the boundary conditions

$$F'(\infty) = 0 = H(\infty) = F(0) = F'(0) = H'(0) + 1. \tag{3}$$

In the limit $\sigma \to \infty$, it can be readily verified that there exists an inner region, corresponding to $\eta = O(\sigma^{-\frac{1}{5}})$, wherein the inertial effect is negligible, and an outer region, corresponding to $\eta = O(\sigma^{-\frac{3}{10}})$, wherein the temperature variable H is identically zero; in both regions, the vertical component of velocity, $F'(\eta)$, is $O(\sigma^{-\frac{3}{5}})$. Hence, introducing the inner and outer variables,

$$\xi \equiv \sigma^{\frac{1}{5}}\eta, \quad \zeta \equiv \sigma^{-\frac{3}{10}}\eta, \tag{4}$$

appropriate asymptotic expansions in the two regions are

$$\left.\begin{aligned} F(\eta) &\sim \sigma^{-\frac{1}{5}}[\mathscr{F}_a(\xi) + \sigma^{-\frac{1}{2}}\mathscr{F}_b(\xi) + \sigma^{-1}\mathscr{F}_c(\xi) + \ldots] \\ H(\eta) &\sim \sigma^{-\frac{1}{5}}[\mathscr{H}_a(\xi) + \sigma^{-\frac{1}{2}}\mathscr{H}_b(\xi) + \sigma^{-1}\mathscr{H}_c(\xi) + \ldots] \end{aligned}\right\} \quad (\xi \text{ fixed}, \sigma \to \infty), \tag{5}$$

$$\left.\begin{aligned} F(\eta) &\sim \sigma^{-\frac{3}{10}}[f_a(\zeta) + \sigma^{-\frac{1}{2}}f_b(\zeta) + \sigma^{-1}f_c(\zeta) + \ldots] \\ H(\eta) &\equiv 0 \end{aligned}\right\} \quad (\zeta \text{ fixed}, \sigma \to \infty). \tag{6}$$

In particular, the governing equations for the leading-order terms are

$$\mathscr{F}_a''' + \mathscr{H}_a = 0, \quad \mathscr{H}_a'' + 4\mathscr{F}_a\mathscr{H}_a' - \mathscr{F}_a'\mathscr{H}_a = 0, \tag{7}$$

$$f_a''' + 4f_a f_a'' - 3f_a' f_a' = 0, \tag{8}$$

subject to the boundary conditions

$$\mathscr{F}_a(0) = 0 = \mathscr{F}_a'(0) = \mathscr{H}_a'(0) + 1 = f_a'(\infty) \tag{9}$$

and the matching conditions

$$\mathscr{F}_a''(\infty) = 0 = \mathscr{H}_a(\infty) = f_a(0), \quad f_a'(0) = \mathscr{F}_a'(\infty). \tag{10}$$

By employing (7) together with the first three conditions in (9) and the first two in (10), it is possible to solve (numerically) for $\mathscr{F}_a$ and $\mathscr{H}_a$ directly; f_a can then be determined and the process continued to obtain $\mathscr{F}_b, \mathscr{H}_b$, etc. However, only results will be presented below since, except for different Prandtl number factors (due to

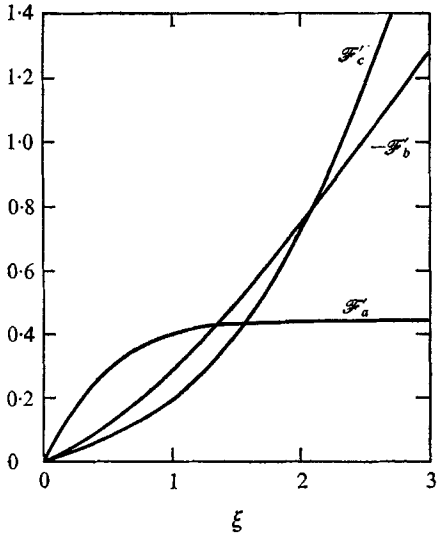

FIGURE 1

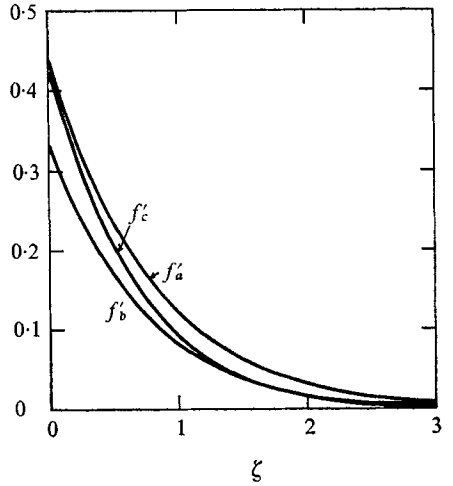

FIGURE 2

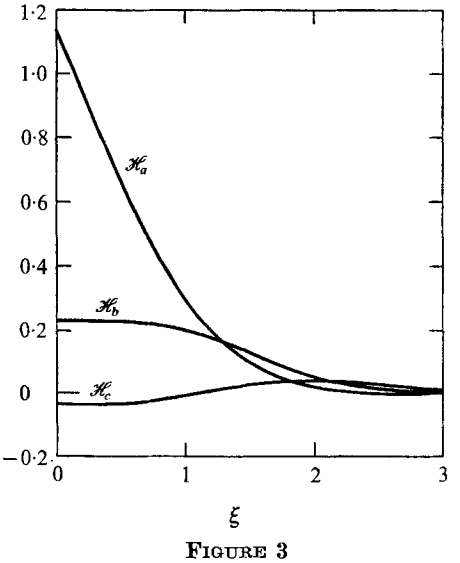

FIGURE 3

FIGURE 1. First three terms in inner expansion for F'.

FIGURE 2. First three terms in outer expansion for F'.

FIGURE 3. First three terms in inner expansion for H.

different characteristic quantities), the present problem is completely analogous to that of the isothermal plate which was solved, to first-order, by LeFevre (1956) and by Stewartson & Jones (1957) and, to third-order, by Kuiken (1968).

The pertinent results with regard to the drag and heat-transfer coefficients are

$$F''(0) \sim \sigma^{-\frac{2}{5}}(0{\cdot}81185 - 0{\cdot}17007\sigma^{-\frac{1}{2}} + 0{\cdot}14131\sigma^{-1} + \ldots), \tag{11}$$

$$H(0) \sim \sigma^{-\frac{1}{5}}(1{\cdot}14744 + 0{\cdot}22594\sigma^{-\frac{1}{2}} - 0{\cdot}03216\sigma^{-1} + \ldots). \tag{12}$$

Concerning the total flow within the boundary layer, we note that

$$F(\infty) \sim \sigma^{-\frac{3}{10}}(0{\cdot}34219 + 0{\cdot}03557\sigma^{-\frac{1}{2}} - 0{\cdot}31666\sigma^{-1} + \ldots). \tag{13}$$

Numerical results for F' and H are shown graphically in figures 1–3.

3. Conjectures

Based upon the results of the preceding section, it seems reasonable to attribute the disparate frequencies associated with modes I and II to different wavelengths, one being characterized by the thickness of the outer layer ($\sim \sigma^{-\frac{3}{10}}\delta$), the other by the inner-layer thickness ($\sim \sigma^{-\frac{1}{5}}\delta$). Noting also that, in both cases, the speed of propagation of the disturbance wave is proportional to the primary flow speed ($\sim \sigma^{-\frac{2}{5}}U$, where $U \equiv (\nu/5x)\,G^{*2}$ characterizes the speed of the fluid when σ is $O(1)$) and the non-dimensionalized frequencies associated with mode I are smaller than those of mode II, we conjecture that the characteristic frequencies of modes I and II are, respectively, $(U/\delta)\,\sigma^{-\frac{9}{10}}$ and $(U/\delta)\,\sigma^{-\frac{2}{5}}$.

Determination of the G^* régime associated with each mode is less straightforward. From the results in (A), however, one notes that the unstable region of mode I (or the associated uncoupled mode) corresponds to much larger values of G^* than that of II. We will assume that modes I and II correspond, respectively, to $G^* = O(\sigma^{\frac{13}{10}})$ and to $O(\sigma^{\frac{3}{10}})$; the reason for such limiting behaviours will become clear from the analysis in §§ 4 and 5.

Employing the above results, the large Prandtl number neutral stability curves obtained in (A) have been rescaled (in terms of σ) in figures 4–5. The curves in figure 4 are for the uncoupled case (associated with mode I), those in 5 for mode II. In both cases, the curves appear to approach a definite limit as σ increases, substantiating the dependences conjectured above.

4. Mode II

On the basis of § 3, we introduce the following $O(1)$ quantities:

$$S \equiv \sigma^{-\frac{3}{10}}G^*, \quad \Omega \equiv \sigma^{\frac{2}{5}}\omega\delta/U,$$

(ω being the physical frequency of the disturbance) and the following asymptotic expansions:

$$\alpha \sim \sigma^{\frac{1}{5}}(\alpha_a + \sigma^{-\frac{1}{2}}\alpha_b + \ldots), \quad c \sim \sigma^{-\frac{3}{5}}(c_a + \sigma^{-\frac{1}{2}}c_b + \ldots), \tag{14}$$

where $\alpha \equiv \delta\, d\gamma/dx$ and $c \equiv \omega\delta/U\alpha$ are complex, the real part of α being the non-dimensional disturbance wave-number and the real part of c being approximately

equal to the non-dimensionalized wave speed. Hence, appropriate expansions for the disturbance field are

$$\left.\begin{aligned}\phi &\sim \sigma^{-\frac{1}{6}}[\Phi_a(\xi)+\sigma^{-\frac{1}{2}}\Phi_b(\xi)+\ldots],\\ \theta &\sim \sigma^{\frac{2}{3}}[\Theta_a(\xi)+\sigma^{-\frac{1}{2}}\Theta_b(\xi)+\ldots],\end{aligned}\right\} \quad (\xi,\ S \text{ and } \Omega \text{ fixed},\ \sigma\to\infty), \tag{15}$$

where ϕ and θ are the non-dimensionalized disturbance stream function and temperature defined in (A). The arbitrary scale of the disturbance field has been fixed by choosing the velocity components to be $O(1)$.

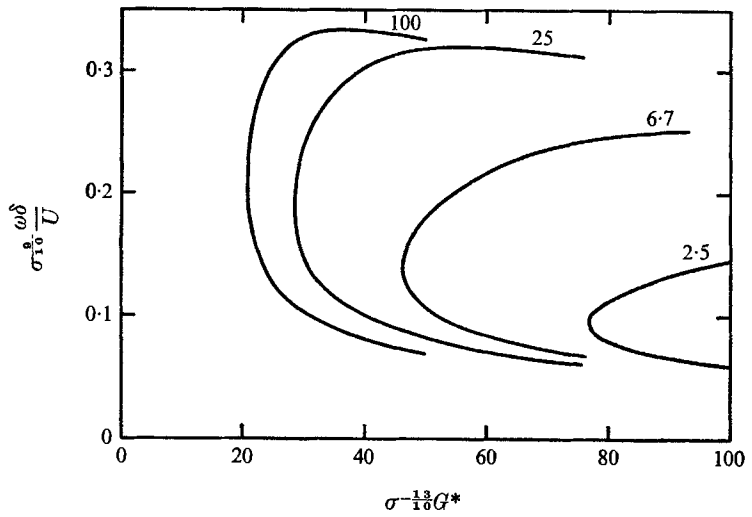

FIGURE 4. Uncoupled neutral stability curves at σ = 2·5, 6·7, 25, 100.

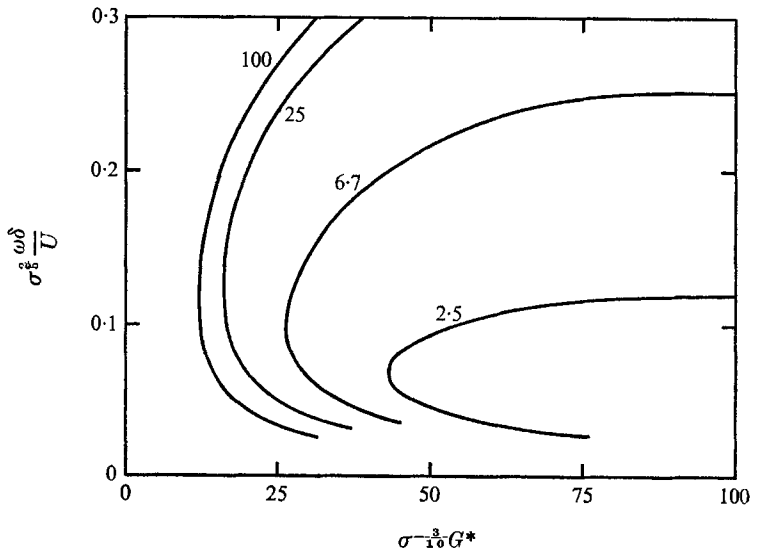

FIGURE 5. Nose region of coupled neutral stability curves at σ = 2·5, 6·7, 25, 100; $\theta(0)$ = 0.

We recall from (A) that the governing equations for the disturbance field are

$$(F'-c)(\phi''-\alpha^2\phi)-F'''\phi = (1/i\alpha G^*)(\phi^{\mathrm{iv}}-2\alpha^2\phi''+\alpha^4\phi+\theta'), \tag{16}$$

$$(F'-c)\theta-H'\phi = (1/i\alpha\sigma G^*)(\theta''-\alpha^2\theta), \tag{17}$$

subject to the boundary conditions:

$$\phi(\infty) = 0 = \phi'(\infty) = \theta(\infty) = \phi(0) = \phi'(0) = \theta(0) \quad \text{or} \quad \theta'(0). \tag{18}$$

By assuming $\alpha = O(\sigma^{\frac{1}{2}})$ and noting that $d/d\eta = O(\sigma^{-\frac{3}{10}})$ in the outer region, it follows directly from (16)–(18) that the disturbance field must be identically zero in the outer layer. That is, the assumption that the wavelength is of the order of the thickness of the inner layer implies that the disturbance field is restricted to the inner region.

Substituting (14)–(15) into (16)–(17) results in the following governing equations for the first two terms in (15):

$$\mathscr{L}(\Phi_a) \equiv \Phi_a^{\mathrm{iv}}-2\alpha_a^2\Phi_a''+\alpha_a^4\Phi_a+(\mathscr{H}_a'\,\Phi_a/(\mathscr{F}_a'-c_a))' = 0, \tag{19}$$

$$\mathscr{L}(\Phi_b) = iS\chi_1+iS^{-1}\chi_2+\alpha_b\chi_3+\chi_4 \equiv Q, \tag{20}$$

where Θ_a, Θ_b have been eliminated via the disturbance energy equation and where

$$\chi_1 \equiv \alpha_a[(\mathscr{F}_a'-c_a)(\Phi_a''-\alpha_a^2\Phi_a)-\mathscr{F}_a'''\Phi_a],$$

$$\chi_2 \equiv \alpha_a^{-1}[(\Theta_a''-\alpha_a^2\Theta_a)/(\mathscr{F}_a'-c_a)]' \quad \text{with} \quad \Theta_a = \mathscr{H}_a'\,\Phi_a/(\mathscr{F}_a'-c_a),$$

$$\chi_3 \equiv 4\alpha_a\Phi_a''-4\alpha_a^3\Phi_a+c_a\alpha_a^{-1}[\Theta_a/(\mathscr{F}_a'-c_a)]',$$

$$\chi_4 \equiv [(\mathscr{F}_b'\,\Theta_a-\mathscr{H}_b'\,\Phi_a)/(\mathscr{F}_a'-c_a)]'.$$

The appropriate boundary conditions for (19)–(20) are

$$\Phi_j(0) = 0 = \Phi_j'(0) = \Phi_j(\infty) = \Phi_j'(\infty) \quad (j = a, b). \tag{21}$$

Physically, (19) indicates that, in the zeroth-order approximation, viscous diffusion of vorticity is balanced by the buoyancy effect with the convection of vorticity being of smaller order. In addition, the result for Θ_a indicates that thermal diffusion is of smaller order than thermal convection. In (20), the terms $iS\chi_1$ and $iS^{-1}\chi_2$ are due, respectively, to the convection of vorticity and the diffusion of thermal energy; that these effects are of first order (i.e. $O(\sigma^{-\frac{1}{2}})$ smaller than the leading-order terms), is a consequence of assuming $G^* = O(\sigma^{\frac{3}{10}})$.

It is noted that the limiting equations, (19)–(21), are of the same form as those obtained by Gill & Davey (1969) in their large Prandtl number stability analysis of a 'buoyancy layer' (i.e. the one-dimensional flow arising from a doubly-infinite vertical plate heated to a uniform temperature excess relative to a linearly stratified external temperature field), which is a much simpler primary flow in that its structure is independent of σ. As a result, the solution of (19)–(21) is qualitatively similar to that of the above paper and, therefore, will only be presented in condensed form, the reader being referred to Gill & Davey for further details.

Results for α_a and c_a versus Ω are shown in figure 6, the eigenvalue (α_a) being obtained by numerical integration of (19) subject to the boundary conditions in (21). It is noted that $c_a > (\mathscr{F}_a')_{\max}$, assuring that the operator $\mathscr{L}$ is not singular.

Since α_a is real, indicating neutral stability to this order of approximation, α_b must be evaluated in order to determine the unstable régime.

From (20)–(21) one obtains the requirement that

$$\int_0^\infty \psi Q \, d\xi \equiv \langle \psi, Q \rangle = 0, \tag{22}$$

where ψ is a non-trivial solution of the adjoint problem

$$\psi^{\mathrm{iv}} - 2\alpha_a^2 \psi'' + \alpha_a^4 \psi - (\mathscr{H}_a' \psi')/(\mathscr{F}_a' - c_a) = 0; \; \psi(0) = 0 = \psi'(0) = \psi(\infty) = \psi'(\infty).$$

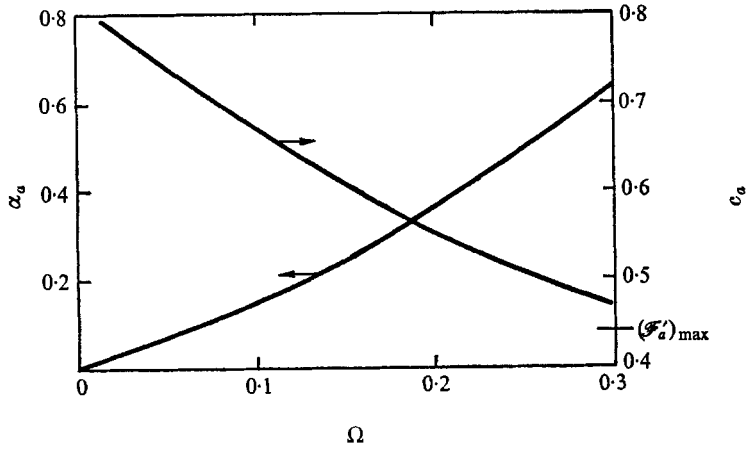

FIGURE 6. Values of α_a and c_a; mode II.

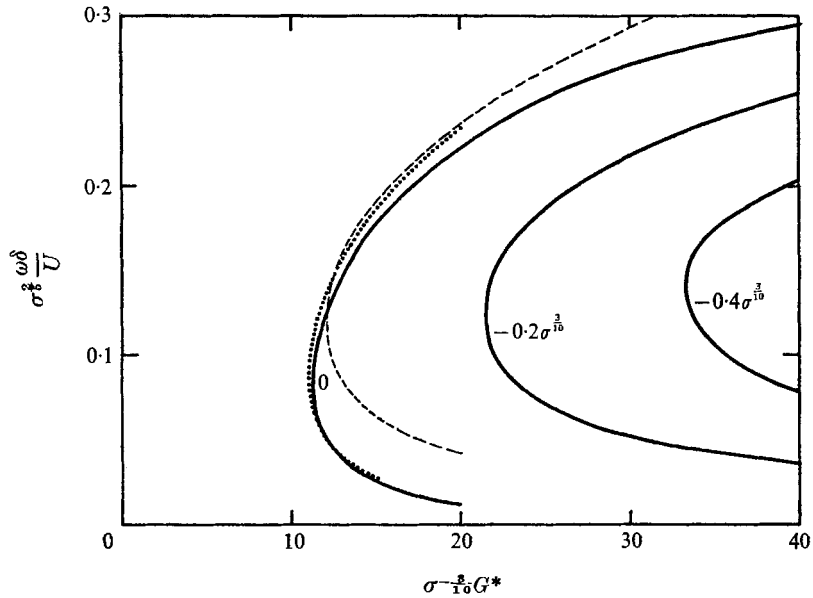

FIGURE 7. Contours of constant values of α_i for mode II; dashed and dotted contours are neutral stability curves at $\sigma = 100$ for $\theta(0) = 0$ and $\theta'(0) = 0$, respectively.

In particular, the imaginary part of (22) results in

$$-(\alpha_b)_i = (\langle\psi,\chi_1\rangle/\langle\psi,\chi_3\rangle)\,S + (\langle\psi,\chi_2\rangle/\langle\psi,\chi_3\rangle)\,S^{-1}. \tag{23}$$

Noting that $\alpha_i \sim \sigma^{-\frac{3}{16}}(\alpha_b)_i$, results based upon (23) are shown graphically in figure 7.

Throughout the present analysis, no consideration has been given to the boundary conditions on θ. Accordingly, we note that the quantity

$$\Theta_a = \mathscr{H}_a'\,\Phi_a/(\mathscr{F}_a' - c_a)$$

vanishes at infinity and satisfies the boundary condition at the wall, whether it be $\Theta_a(0) = 0$ or $\Theta_a'(0) = 0$. On the other hand, the solution for Θ_b (implicit in (20)), while vanishing at infinity, is non-zero and has a non-zero first derivative at the wall. This complication is resolved by noting that, by reducing the sixth-order governing equations, (16)–(17), to the fourth-order limiting equations such as (20), we have neglected the 'viscous coupled' integral, ϕ_3 (in the notation of (A)). The latter is exponentially small except for the thin region, $\eta = O(\sigma^{-\frac{9}{20}})$, wherein $\theta_3/\phi_3 = O(\sigma^{\frac{27}{20}})$. Hence, by adding an appropriate multiple of (ϕ_3, θ_3) to the above solutions, the temperature boundary condition at the wall can be satisfied without affecting the disturbance velocity field (to the order of the above analysis). Therefore, the results based upon (23) are applicable to both cases: $\theta(0) = 0$ and $\theta'(0) = 0$. This is corroborated in figure 7 where the neutral stability curve at $\sigma = 100$ has been included for these two cases.

5. Mode I (or uncoupled mode)

Employing the results of § 3, we introduce the quantities:

$$R \equiv \sigma^{-\frac{13}{16}}G^*, \quad \Lambda \equiv \sigma^{\frac{9}{16}}\omega\delta/U,$$

and the asymptotic expansions

$$\alpha \sim \sigma^{-\frac{3}{16}}(\alpha_a + \sigma^{-\frac{1}{2}}\alpha_b + \sigma^{-1}\alpha_c + \ldots), \quad c \sim \sigma^{-\frac{3}{8}}(c_a + \sigma^{-\frac{1}{2}}c_b + \sigma^{-1}c_c + \ldots). \tag{24}$$

Restricting attention first to the uncoupled case, it follows that appropriate outer and inner expansions for the disturbance field are, respectively,

$$\phi \sim \sigma^{\frac{3}{16}}[\phi_a(\zeta) + \sigma^{-\frac{1}{2}}\phi_b(\zeta) + \sigma^{-1}\phi_c(\zeta) + \ldots], \quad (\zeta, R \text{ and } \Lambda \text{ fixed}, \sigma \to \infty), \tag{25}$$

$$\phi \sim \sigma^{-\frac{1}{8}}[\Phi_a(\xi) + \sigma^{-\frac{1}{2}}\Phi_b(\xi) + \sigma^{-1}\Phi_c(\xi) + \ldots], \quad (\xi, R \text{ and } \Lambda \text{ fixed}, \sigma \to \infty). \tag{26}$$

Substituting (6), (24) and (25) into the uncoupled disturbance vorticity equation ((16) with the term $\theta'/i\alpha G^*$ omitted), one obtains the following governing equation for ϕ_a:

$$\mathscr{L}_1(\phi_a) \equiv (f_a' - c_a)(\phi_a'' - \alpha_a^2\phi_a) - f_a''\phi_a = 0. \tag{27}$$

Similarly, employing (5), (24) and (26), the governing equation for Φ_a becomes

$$i\alpha_a R[(\mathscr{F}_a' - c_a)\,\Phi_a'' - \mathscr{F}_a'''\Phi_a] = \Phi_a^{\mathrm{iv}}. \tag{28}$$

These functions must satisfy the boundary conditions:

$$\phi_a(\infty) = 0 = \Phi_a(0) = \Phi_a'(0), \tag{29}$$

together with the matching conditions:

$$\phi_a(0) = 0 = \Phi_a''(\infty), \quad \Phi_a'(\infty) = \phi_a'(0). \tag{30}$$

We note that the problem for ϕ_a, consisting of equation (27) and the first condition in each of (29) and (30), is merely the inviscid stability problem. Since the profile of f_a' (indicated in figure 2) does not contain an inflexion point, it follows from a well-known result in stability theory that the flow is stable, i.e. $(\alpha_a)_i > 0$. The actual values of $(\alpha_a)_i$ and $(c_a)_r$ are shown in figure 8. These results were obtained by guessing a value for α_a at a given Λ and then integrating (27) along the complex ζ contour indicated in figure 8, beginning with $\phi_a(\xi) = e^{-\alpha_a \zeta}$ at the edge of the outer layer; α_a was then iterated upon until $\phi_a = 0$ at $\zeta = 0$.

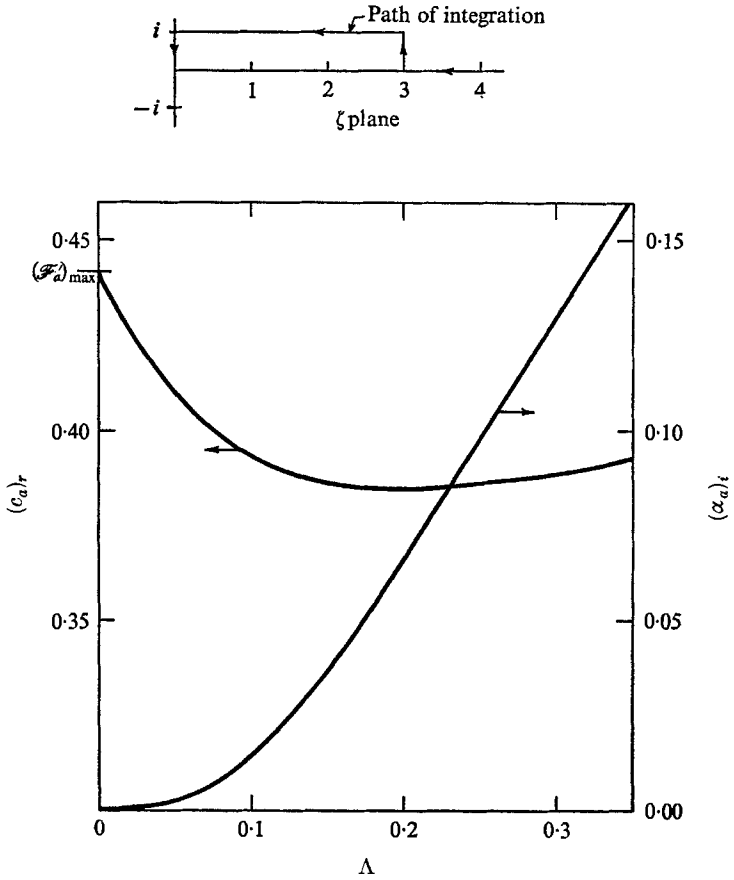

FIGURE 8. Values of $(\alpha_a)_i$ and $(c_a)_r$ for uncoupled mode.

On the basis of the first term in the expansion for α, it is seen that the uncoupled mode is stable for sufficiently large σ. However, since figure 4 indicates that the uncoupled mode is unstable at $\sigma = 100$, it follows that the higher-order terms in the expansion for α must predominate even at this large value of σ. It is therefore desirable to obtain these higher-order terms; this necessitates first determining Φ_a.

Since ϕ_a and α_a have been obtained for given Λ ($=\alpha_a c_a$), Φ_a can be determined by solving (28) subject to the last two conditions in each of (29) and (30). (It is noted that the term on the right-hand side of (28) is due to viscous diffusion of vorticity, Φ_a in effect being a viscous correction which is required in order to satisfy the non-slip condition at the wall. That the convection and diffusion of vorticity are of the same order in the inner region, is a consequence of assuming $G^* = O(\sigma^{\frac{13}{10}})$.) In particular, as $\xi \to \infty$, $\mathscr{F}_a'$ approaches a positive constant (γ_1, say) and $\mathscr{F}_a'''$ is exponentially small; hence,

$$\Phi_a(\xi) \sim A_1\xi + A_0 + A_2 e^{-\gamma_2\xi} \quad (\xi \to \infty), \tag{31}$$

where $A_1 = \phi_a'(0)$ and $\gamma_2 \equiv [i\alpha_a R(\gamma_1 - c_a)]^{\frac{1}{2}}$ with $(\gamma_2)_r > 0$. Starting with (31) at the edge of the inner layer, one then numerically integrates (28) into the wall, iterating on A_0 and A_2 until $\Phi_0(0)$ and $\Phi_a'(0)$ are zero.

Proceeding to the second term in the outer expansion, the governing equation is

$$\mathscr{L}_1(\phi_b) = g_1(\zeta) + \alpha_b g_2(\zeta), \tag{32}$$

where $\mathscr{L}_1$ is the inviscid operator defined in (27) and

$$g_1 \equiv f_b'''\phi_a - f_b'(\phi_a'' - \alpha_a^2\phi_a),$$
$$g_2 \equiv 2\alpha_a(f_a' - c_a)\phi_a - (c_a/\alpha_a)(\phi_a'' - \alpha_a^2\phi_a).$$

(In obtaining g_2, use has been made of the relation: $c_b = -\alpha_b c_a/\alpha_a$.) The boundary conditions on ϕ_b are

$$\phi_b(\infty) = 0, \quad \phi_b(0) = A_0, \tag{33}$$

the second condition in (33) arising from matching requirements.

By considering the behaviour of g_1 and g_2 for large ζ, one has from (32) that

$$\phi_b \sim \alpha_b(-\zeta e^{-\alpha_a\zeta}) + B_1 e^{-\alpha_a\zeta}, \tag{34}$$

the smaller-order terms, arising from g_1, having been omitted in (34). Since we have fixed the arbitrary scale of the disturbance field by taking $\phi \sim \sigma^{\frac{3}{10}} e^{-\alpha_a\zeta}$ as $\zeta \to \infty$, B_1 is therefore zero. Hence, the procedure is to start with (34) at the edge of the outer layer and to numerically integrate (32) along the path indicated in figure 8, iterating on α_b until $\phi_b(0) = A_0$.

It is noted that although R does not appear in the governing equation for ϕ_b, α_b and ϕ_b are still dependent upon R via the matching condition, A_0 being a function of R and Λ. Hence, the leading effect of viscosity upon the stability of the flow arises from the non-zero horizontal velocity component at the edge of the inner viscous layer which influences the second term in the outer region via matching considerations.

Numerical results for $(\alpha_b)_i$ are presented in figure 9, the curves being for fixed values of R. As expected, $(\alpha_b)_i$ is negative, indicating instability. In particular, by comparing figures 8 and 9 it is seen that, at $\sigma = 100$, $\sigma^{-\frac{9}{10}}(\alpha_b)_i$ predominates over $\sigma^{-\frac{9}{10}}(\alpha_a)_i$ for almost all the values of (Λ, R) shown. Although this is in qualitative agreement with the curve in figure 4 for $\sigma = 100$, it is clear that the first two terms in the expansion for α are inadequate at $\sigma = 100$, as can be seen by noting that the two terms predict the flow to be unstable at $R = 10$ for the indicated values of Λ.

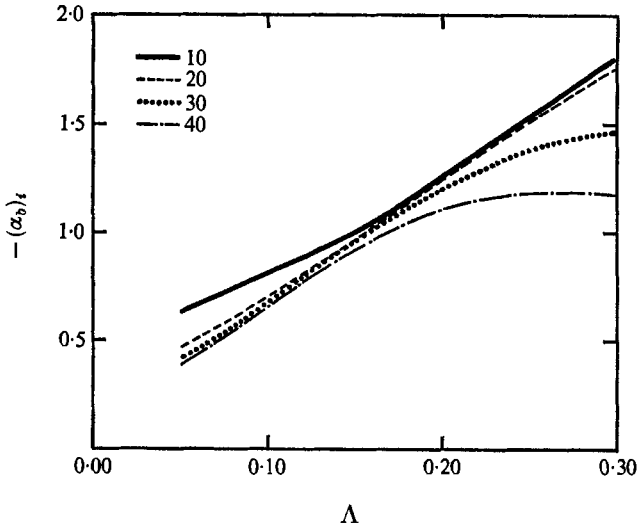

FIGURE 9. Values of $(\alpha_b)_i$ for uncoupled mode; curves correspond to constant values of R.

In order to shed some light upon the expansion for α, we proceeded to determine the third term, $\sigma^{-\frac{13}{16}}\alpha_c$. This necessitated obtaining the second inner, Φ_b, and then the third outer, ϕ_c. Since the details are laborious but straightforward, we will only present the results for $(\alpha_c)_i$, indicated in figure 10.

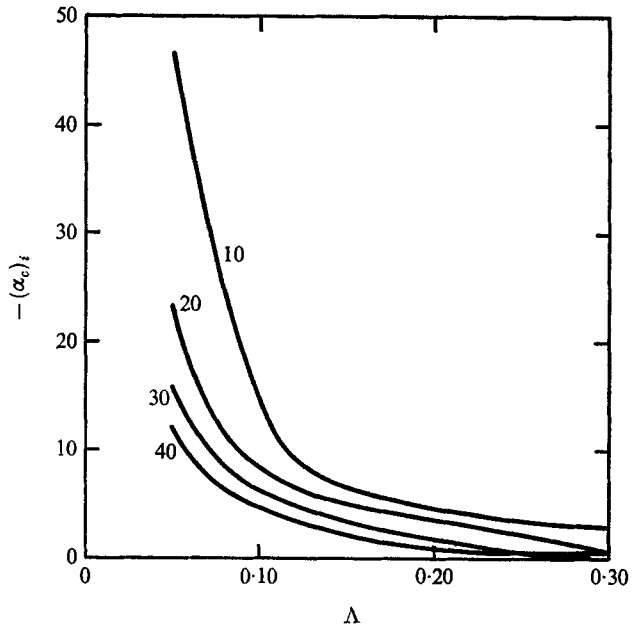

FIGURE 10. Values of $(\alpha_c)_i$ for uncoupled mode; curves correspond to constant values of R.

It is immediately evident that the series expansion for α is, at best, slowly convergent, particularly for small values of R and Λ. The strongest conclusion which seems warranted is that, for R and Λ fixed, the flow becomes stable as $\sigma \to \infty$; clearly, this limiting behaviour is not uniform in R and Λ. This is substantiated by figure 11 wherein the uncoupled neutral stability curves are shown at $\sigma = 100$, 400, 1600 and 6400.

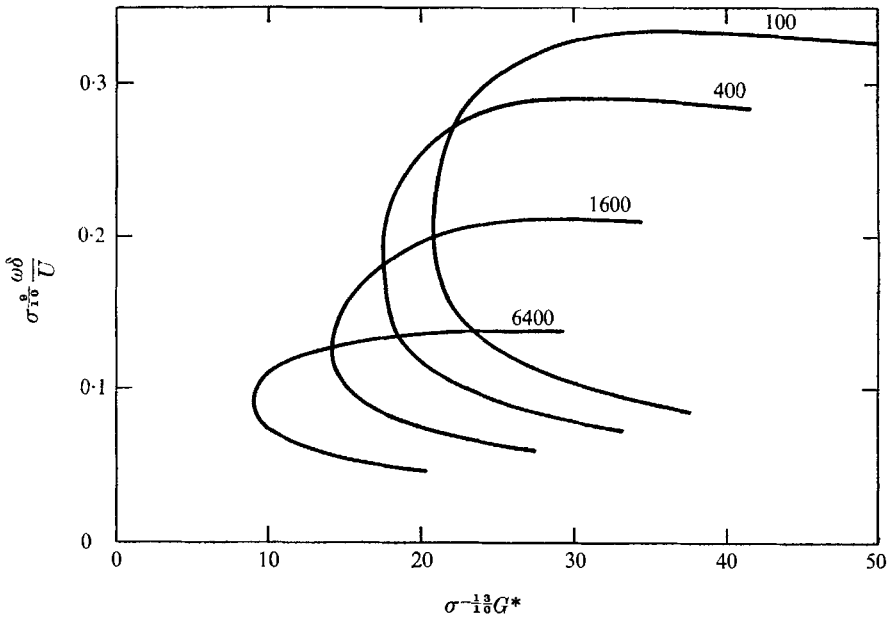

FIGURE 11. Uncoupled neutral stability curves at $\sigma = 100$, 400, 1600, 6400.

Concerning the associated coupled case (mode I), it is noted that θ is identically zero in the outer region and that an appropriate expansion in the inner region is

$$\theta \sim \sigma^{\frac{2}{3}}[\Theta_a(\xi) + \sigma^{-\frac{1}{2}}\Theta_b(\xi) + \ldots] \quad (\xi, R \text{ and } \Lambda \text{ fixed}, \sigma \to \infty).$$

As a result, the governing equation and boundary conditions on ϕ_a are the same as for the uncoupled case, indicating that the results for $(\alpha_a)_i$ shown in figure 8 also apply to mode I. On the other hand, the governing equation for Φ_a reduces to (28) with the additional term,

$$\Theta_a' = (\mathscr{H}_a' \, \Phi_a/(\mathscr{F}_a' - c_a))',$$

appearing on the right-hand side. As a result, α_b for mode I differs from that of the uncoupled case but has the same value for either $\theta(0) = 0$ or $\theta'(0) = 0$. Since the determination of α_b and α_c in the uncoupled case was of rather marginal value, we will desist from a similar determination for mode I. The point to note is that the theory indicates that mode I is indeed associated with the uncoupled problem, as was surmised from the results in (A).

6. Some observations

The results of the previous sections indicate that, as $\sigma \to \infty$, the vertical natural convection boundary layer first becomes unstable when $G^* = O(\sigma^{\frac{3}{10}})$, the instability being associated with the inner (thermal) layer of the primary flow. It is noted, however, that the validity of the boundary-layer approximation is limited by the requirement that the outer layer correspond to $y/x < O(1)$ or, since $\zeta = \sigma^{-\frac{3}{10}}\eta \sim yG^*/x\sigma^{\frac{3}{10}}$, that $G^* > O(\sigma^{\frac{3}{10}})$. This appears to bring into question the self-consistency of the stability analysis for mode II. (For example, at $G^*\sigma^{-\frac{3}{10}} = 11{\cdot}4$, corresponding to the nose of the neutral stability curve in

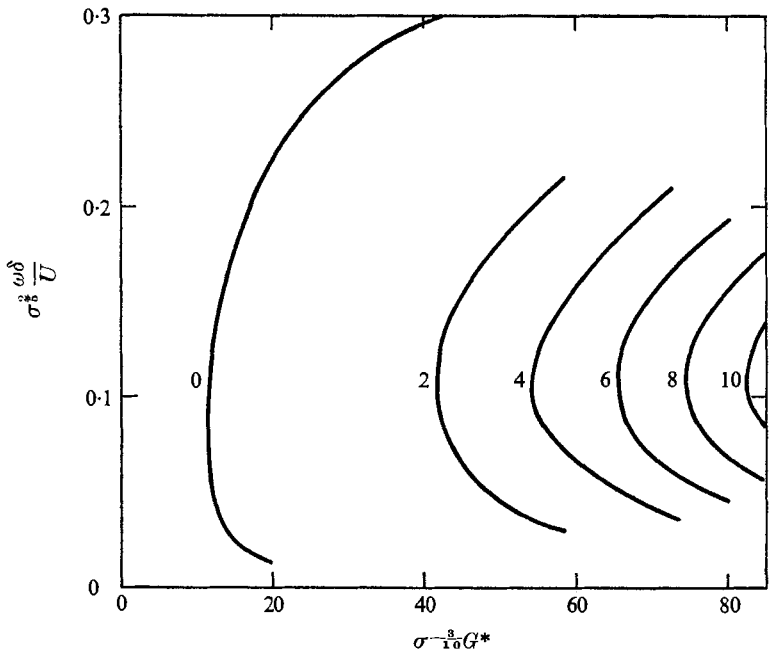

FIGURE 12. Contours of constant values of $-\frac{1}{4}\int\alpha_i dG^*$; mode II.

figure 7, $y/x = 1$ at $\zeta = 11{\cdot}4/5 \simeq 2{\cdot}3$, indicating that the neglect of x-directional diffusion in the outer region is untenable.) The point to be noted, however, is that the stability theory for mode II is concerned solely with the inner region of the primary flow, for which the boundary-layer approximation is certainly valid when $G^* = O(\sigma^{\frac{3}{10}})$. In addition, the outer region does not have a significant effect upon the inner, as is seen by noting that the inner-layer problem, equation (7) subject to the first three conditions in (9) and the first two in (10), is completely self-contained. (More precisely, there is an implicit dependence upon the outer region which arises in considering the propriety of the condition $\mathscr{F}_a''(\infty) = 0$. Physically, this condition is due to the fact that the rate of change (in x) of fluid momentum in the outer layer is of smaller order than the viscous shear force associated with $\mathscr{F}_a''$; hence, since the viscous diffusion in the x direction clearly does not increase the order of magnitude of the inertial effect in the outer region,

the condition $\mathscr{F}_a''(\infty) = 0$ is valid.) We therefore conclude that the stability analysis in § 4 is valid even though it corresponds to a flow régime in which the outer layer of the boundary layer has not yet become fully established.

It is important to note that, although α_i for mode II is $O(\sigma^{-\frac{3}{10}})$, the values of $-\frac{1}{4}\int \alpha_i dG^*$ are $O(1)$. This is indicated in figure 12 where contours of constant values of $-\frac{1}{4}\int \alpha_i dG^*$ are shown. Combining these results with the empirical correlations, obtained in (A), between linear stability theory and experimentally determined régimes of the turbulent-transition process, it follows that, for large σ, we can expect the flow to first become noticeably oscillatory at $G^* \approx 65\sigma^{\frac{3}{10}}$ and the mean (temporal) flow quantities to first deviate significantly from those of laminar flow at $G^* \approx 82\sigma^{\frac{3}{10}}$. This indicates that, for sufficiently large σ, it is mode II which is solely responsible for the turbulent transition of the primary flow. (For example, at $\sigma = 100$, $82\sigma^{\frac{3}{10}} \simeq 325$ whereas the critical value of G^* for the uncoupled neutral curve is ≈ 8200.)

From the above two paragraphs, it follows that the vertical natural convection boundary layer is unstable as $\sigma \to \infty$. That is, we may expect the flow to become turbulent before the two-layer structure of the laminar boundary layer is fully developed. (For example, at $G^* = 82\sigma^{\frac{3}{10}}$, $\zeta = 3$ corresponds to $y/x \simeq \frac{1}{5}$.)

As was found in (A), the cases of an isothermal and a uniform-heat-flux plate can be directly related to each other in terms of G^* or the more familiar Grashof number, G. For the uniform-heat-flux case,

$$G \equiv \frac{g\beta(T_w - T_\infty)x^3}{\nu^2} = \frac{H(0)}{125}(G^*)^4 \sim \frac{\mathscr{H}_a(0)}{125}\sigma^{-\frac{1}{5}}(G^*)^4 \quad (\sigma \to \infty).$$

Then, for example, the inner layer corresponds to $\xi = O(1)$, where

$$\xi \equiv \sigma^{\frac{1}{5}}\eta = \sigma^{\frac{1}{5}}(y/5x)\,G^* \sim (y/x)\,(\sigma G)^{\frac{1}{4}} \quad (\sigma \to \infty),$$

a result which Kuiken (1968) found in a study of the primary flow over an isothermal plate. Similarly, all the remaining characteristic flow quantities of the uniform-heat-flux case can be shown to have the same σ and G dependence as the isothermal case. From this similarity, we can expect the stability properties of the two cases to be at least qualitatively equivalent. In particular, for either case, the unstable regions of modes I and II correspond, respectively, to $G = O(\sigma^5)$ and $G = O(\sigma)$ with the associated wavelength (λ) of the disturbances being

$$\lambda/x = O(\sigma^{-1}) \quad \text{and} \quad \lambda/x = O(\sigma^{-\frac{1}{2}}).$$

The authors wish to acknowledge the support of the National Science Foundation through research Grants GK 1963 and GK 18529.

REFERENCES

GILL, A. E. & DAVEY, A. 1969 Instability of a buoyancy-driven system. *J. Fluid Mech.* **35**, 775–798.

HIEBER, C. A. & GEBHART, B. 1971 Stability of vertical natural convection boundary layers: some numerical solutions. *J. Fluid Mech.* **48**, 625–646.

KNOWLES, C. P. & GEBHART, B. 1968 The stability of the laminar natural convection boundary layer. *J. Fluid Mech.* **34**, 657–686.

KUIKEN, H. K. 1968 An asymptotic solution for large Prandtl number free-convection. *J. Engng. Math.* **2**, 355–371.

LEFEVRE, E. J. 1956 Laminar free convection from a vertical plane surface. *Ninth Int. Congr. Appl. Mech.* (Brussels), **4**, 168–173.

STEWARTSON, K. & JONES, L. T. 1957 The heated vertical plate at high Prandtl number. *J. Aero. Sci.* **24**, 379–380.